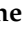




Article

Extending Maximum-Entropy Interbank Reconstruction to a Multi-Country Framework with Cross-Border Exposures

Simone Sbaraglia ¹, Pin Guo ² and Stefano Zedda ^{1,*}

¹ Department of Economics and Business Sciences, University of Cagliari, Via Sant'Ignazio 74, 09123 Cagliari, Italy; sbaraglia@unica.it

² School of Economics and Finance, Xi'an Jiaotong University, Xi'an 710049, China; guopin198961@163.com

* Correspondence: szedda@unica.it

Abstract

Estimating bilateral interbank exposures is essential for assessing systemic risk and contagion in global banking systems. We propose a reconstruction framework that extends the maximum-entropy approach to a multi-country setting by integrating domestic balance-sheet total interbank exposure values with country-level aggregate cross-border exposures. The method distributes each country's external positions across its resident banks and then reconstructs the domestic interbank matrices under maximum-entropy constraints, yielding a globally consistent exposure matrix. Cross-border aggregates—such as those published by the BIS—enter the framework only as optional external constraints rather than as objects of empirical validation. The resulting dual-layer interbank network improves the internal coherence of multi-country exposure estimates and provides a consistent input for contagion simulations and systemic risk analysis.

Keywords: banking system; interbank matrix; systemic risk; international contagion

JEL Classification: G01; G17; G15; G21

1. Introduction and Literature Review

The 2008 global financial crisis propelled the issue of banking systemic risk—characterized by cross-institutional, cross-market, and cross-border transmission—to the policy spotlight (Adrian & Brunnermeier, 2016). Given that contagion effects constitute the primary mechanism for systemic risk materialization (Aldasoro et al., 2015, and as interbank contagion effects are characterized by a knife-edge property (Ladley, 2011), their effective measurement represents a central concern for global scholars and regulators.

Due to differences across countries in market completeness, transparency, and disclosure regimes, existing studies predominantly employ two methodologies to quantify banking systemic risk contagion: network models and market models.¹

Network models primarily utilize bank balance sheet data to construct interbank exposure matrices and then employ multiple simulation shocks to measure contagion effects and systemic risk among banks under various stress scenarios. These models operate on the premise that lending relationships formed through balance sheet positions and interbank transactions create complex debt–credit network structures, which can propagate individual distress throughout the financial system (Allen & Gale, 2000; Freixas et al., 2000, Upper & Worms, 2004). Insolvency at one or several banks may trigger contagion and liquidity shortfalls (Cifuentes et al., 2005; Davidović et al., 2019; Davydov et al., 2021). Researchers



Academic Editor: Thanasis Stengos

Received: 26 December 2025

Revised: 29 January 2026

Accepted: 3 February 2026

Published: 13 February 2026

Copyright: © 2026 by the authors.

Licensee MDPI, Basel, Switzerland.

This article is an open access article distributed under the terms and conditions of the [Creative Commons Attribution \(CC BY\)](https://creativecommons.org/licenses/by/4.0/) license.

such as [Battiston et al. \(2012\)](#), [Huang et al. \(2009\)](#), [Glasserman and Young \(2015\)](#), [Levy-Carciente et al. \(2015\)](#), and [Zedda and Cannas \(2020\)](#) have applied this methodology to measure systemic risk levels in banks across developed and developing economies.

Market models, conversely, use stock price volatility data from financial institutions to quantify tail risk spillover effects between individual institutions and the financial system. Common technical methodologies include Marginal Expected Shortfall (MES) and Conditional Value-at-Risk (CoVaR). [Acharya and Yorulmazer \(2010\)](#) pioneered the MES framework, estimating an institution's marginal systemic risk contribution through its expected return conditional on significant financial system downturns. [Brownlees and Engle \(2017\)](#) incorporated asset size, leverage, and long-run MES (LRMES) to gauge a bank's expected capital shortfall under crisis conditions, treating this shortfall as a systemic risk indicator. Concurrently, [Adrian and Brunnermeier \(2016\)](#) proposed the CoVaR methodology, measuring a bank's marginal systemic risk contribution as the difference between the financial system's CoVaR conditional on that bank's distress versus normal operation. Extending this framework, [Karimalis and Nomikos \(2018\)](#) employ Copula-based CoVaR to identify common market factors that trigger systemic risk and to examine correlations between institutional characteristics (e.g., size, leverage, equity beta) and systemic risk contributions.

Overall, the two aforementioned approaches exhibit complementary strengths and limitations. The network model approach enables simulation of systemic risk generation and contagion processes. Furthermore, its independence from high-frequency stock price volatility data ensures applicability to both listed and non-listed banks in the financial market ([Zhang et al., 2020](#)). Its primary limitation lies in the lower reporting frequency of bank balance sheet data, which impedes the timely measurement of banking systemic risk ([Holopainen & Sarlin, 2017](#)). Conversely, while the market model approach allows timely and up-to-date estimates, its reliance on high-frequency equity data restricts its applicability in less-developed markets or for non-listed banks ([Zedda & Cannas, 2020](#)). As [Brunnermeier et al. \(2009\)](#) emphasize, effective contagion measurement must quantify contributions from both large, systemically important institutions and smaller, non-listed entities—a regulatory imperative underscored by [Benoit et al. \(2017\)](#). Guided by these considerations, this study adopts the balance-sheet-based network model approach.

Notably, existing network-based contagion research overwhelmingly centers on within-country transmission across institutions or markets, while cross-border contagion effects remain under-studied. However, since the 2008 global financial crisis, deepening financial integration has intensified cross-border interbank activity, with a growing body of research demonstrating that capital mobility facilitates the transmission of financial risks between nations, resulting in significant cross-border contagion effects ([Bostanci & Yilmaz, 2020](#); [Zedda & Spinace-Casale, 2021](#)). This implies that focusing solely on risk spillovers and contagion within a single country may lead to a substantial underestimation of the actual risk contribution of individual institutions and, by extension, understatement of the repercussions of financial-sector distress.

Against this backdrop, we address the core research question of how risk contagion effects from individual bank distress can be more accurately quantified, given increasing global financial interconnectedness. More specifically, we ask how to reconstruct a coherent multi-country interbank exposure matrix when only domestic bank-level totals and country-level aggregate cross-border positions are observable.

Theoretical research employed network theory to examine the banking systems, particularly the structural characteristics of interbank matrices. [Allen and Gale \(2000\)](#) and [Freixas et al. \(2000\)](#) investigated banking systems with varying lending patterns, demonstrating that a given shock triggers contagion in some structures but not others. Further

network analyses, such as [Brusco and Castiglionesi \(2007\)](#) and [Hasman and Samartin \(2008\)](#), concluded that “incompletely connected” networks exhibit greater resilience, since “disconnected” structures are more susceptible to contagion than “complete” ones, but the latter prevent contagion from spreading to all banks. Empirically, [Upper \(2011\)](#) reviewed simulation-based studies on the interbank market’s role in propagating financial contagion, necessitated by the scarcity of real-world contagion data. Subsequent work by [Battiston et al. \(2012\)](#), [Zedda et al. \(2014\)](#), [Elliott et al. \(2014\)](#), [Acemoglu et al. \(2015\)](#), and [Zedda and Sbaraglia \(2020\)](#) has established a link between system resilience and the topological structure of the interbank market.

These studies confirm that the interbank matrix structure plays a fundamental role in determining contagion risks, but such matrices are not publicly available for banks or banking groups. This means that the interbank matrix must be estimated in some way. The most considered reference for this estimation is based on the maximum entropy hypothesis, which is to say, on the maximum diversification of the counterparts. Another constraint to be considered is that no bank lends to itself, so the matrix diagonal elements must be set to zero. The combination of these two constraints, maximum entropy and zeros is implemented by the RAS constrained entropy-maximisation algorithm of [Blien and Graef \(1997\)](#) and widely used in the literature (e.g., in [Battiston et al., 2012](#); [Glasserman & Young, 2015](#); [Levy-Carciente et al., 2015](#); [Zedda & Cannas, 2020](#)).

Bank-to-bank exposure mappings are typically accessible only to supervisors, as in [Mistrulli \(2010\)](#), who compares a maximum-entropy estimate with an actual interbank matrix obtained from confidential data of the Italian central bank. The observed matrix is incompletely connected and more resilient to contagion than the fully connected structure implied by maximum-entropy estimation.

However, existing approaches either reconstruct domestic bilateral exposures without incorporating cross-border constraints, or model cross-border contagion only at the aggregate country level without linking international flows to bank-level balance sheets. To our knowledge, no framework currently integrates these two dimensions to obtain a globally consistent multi-country exposure matrix. Taken together, these contributions show that while domestic interbank structures have been widely analyzed, existing approaches cannot capture how domestic fragilities interact with cross-border exposures—an increasingly important driver of systemic risk.

Typically, due to the lack of more detailed information, the domestic interbank matrix is estimated under a maximum-entropy hypothesis, i.e., assuming maximum diversification of counterparties.

Although some multi-country studies base their estimations on the same maximum-diversification assumption (e.g., [Benczur et al., 2017](#)), this hypothesis is not supported by the BIS country-to-country interbank exposure data. Instead, the availability of the BIS country-to-country interbank exposures mapping allows for a more precise estimation of the international interbank matrix, which can be integrated with the domestic exposure data or estimations.

To fill this gap, we combine features of previous domestic interbank network estimations based on the RAS constrained entropy-maximisation algorithm of [Blien and Graef \(1997\)](#) with the international contagion model of [Zedda and Spinace-Casale \(2021\)](#). The resulting algorithm integrates total exposures (i.e., interbank credits and debts) from financial statements with international country-to-country exposures from the BIS, improving the quality of the interbank matrix approximation and enabling more precise contagion estimates.

This integration constructs a dual-layer interbank network, overcoming traditional models’ country-segmentation assumption while embedding institutional characteristics

within a global financial interconnectedness framework. Consequently, it enables more accurate quantification of both individual bank contagion effects and resultant systemic risk levels.

In this way, we make a significant contribution to the prior literature by explicitly integrating cross-border contagion and providing a more reliable quantification of the contagion risks arising from the distress of individual banks, amid intensifying interlinkages among global financial institutions and markets.

Although the BIS country-to-country exposures can be used as cross-border aggregates within our framework, the methodological contribution of the paper is independent of that specific dataset, and can be applied to any other source providing country-to-country banking exposures. The BIS matrix simply provides a convenient and widely used source of aggregate foreign exposures but is not the object of empirical validation in this work.

The focus of the paper is methodological. While country-level aggregates such as BIS exposures can be used as inputs to the framework, empirical calibration and validation fall outside the scope of this study. The numerical example in Section 3 is therefore designed solely to demonstrate the internal consistency and functioning of the multi-country reconstruction algorithm.

The remainder of this paper is structured as follows. Section 2 describes the multi-country interbank model, Section 3 provides an example of the model application, and Section 4 concludes the paper.

2. Multi-Country Interbank Model

This section sets out the conceptual structure of the multi-country reconstruction framework. The objective is to obtain a fully specified bilateral exposure matrix consistent with (i) bank-level domestic totals and (ii) aggregate cross-border positions. The framework extends the classical maximum-entropy approach by adding country-level constraints that must be reconciled across domestic blocks. This requires allocating each country's external exposures to resident banks in a manner consistent with balance-sheet totals—a step that is absent in single-country models. The approach is therefore not only an implementation procedure but a modelling principle: domestic maximum-entropy estimates are embedded within a global constraint system to produce a coherent multi-country network.

This study investigates how an exogenous shock propagates through a network of mutually exposed banks and may escalate into systemic default. While the literature has long analysed contagion within a single jurisdiction—typically by reconstructing an $n \times n$ interbank liability matrix from bank-level totals and simulating shock cascades—we extend the framework to a multi-country setting. Each country hosts a distinct subset of banks, yet aggregate cross-border positions link countries among themselves.

For a single country, the inputs consist of an $n \times 2$ matrix: column 1 lists each bank's total interbank debts $(d_i)_{i=1}^n$, and column 2 its total interbank credits $(s_i)_{i=1}^n$. The maximum-entropy algorithm then fills the interior of the unknown liability matrix so that row and column sums match the observed totals while the diagonal is forced to zero (banks do not lend to themselves). The resulting matrix supplies all bilateral exposures needed by the downstream contagion engine.

Moving to k countries complicates matters. We now observe k country-level input tables—one per country—plus a $(k + 1) \times (k + 1)$ international exposure matrix $\Gamma = (\gamma_{c,d})$. Entry $\gamma_{c,d}$ is the aggregate liability of country c towards country d ; the final row and column represent the external rest-of-the-world (RoW) and ensure that row totals need not equal column totals when the observable universe of countries is incomplete.

The algorithm developed here transforms those inputs into a single $(N + 2) \times (N + 2)$ matrix \mathcal{L} (with $N = \sum_c n_c$ and n_c the total number of banks in country c) suitable for conta-

gion analysis. First, every country-to-country exposure $\gamma_{c,d}$ is allocated across individual banks of the debtor country in proportion to their domestic liability shares (Section 2.2). Second, the foreign parts are subtracted from the original bank totals, yielding revised domestic row and column vectors (Section 2.3). Third, the maximum-entropy procedure is applied separately to each country on these revised totals, producing domestic blocks $L^{(c)}$ that include a domestic RoW row and column to absorb unobserved resident counterparties (Section 2.4). Fourth, (Section 2.5), bilateral foreign liabilities between banks in different countries are distributed by weighting each bank’s foreign total by

- (i) The share of $\gamma_{c,d}$ in the debtor country’s foreign portfolio;
- (ii) The creditor bank’s share of domestic credits.

Finally, the diagonal domestic blocks, the off-diagonal foreign blocks, and the two RoW layers are assembled into the block matrix \mathcal{L} (Section 2.6). For the illustrative workbook containing three countries and nine explicit banks, the procedure outputs an 11×11 matrix whose structure reproduces precisely all observed aggregates and therefore constitutes a coherent input for subsequent shock-propagation experiments.

2.1. Notation and Input Data

The reconstruction relies on three modelling assumptions.

- (1) Domestic bilateral exposures are unobserved and are therefore approximated by the maximum-entropy solution conditional on revised row/column totals.
- (2) Cross-border aggregates represent binding constraints but do not specify bank-to-bank international exposures; these must be inferred proportionally from observable domestic balance-sheet shares.
- (3) Countries that are outside the sample or have missing reporting are represented through the rest-of-the-world (RoW) layers, ensuring accounting consistency. These assumptions are consistent with existing single-country reconstruction methods but extend them to accommodate multi-country balance-sheet constraints.

For every bank $i \in B_c$ two scalars are observed, where B_c is the set of banks in country c :

$$d_i^{(c)} \text{ (row total : inter-bank debts), } s_i^{(c)} \text{ (column total : inter-bank credits).} \tag{1}$$

They are stored in the country c totals worksheet as two adjacent columns. The country-level aggregate vectors are

$$d^{(c)} = (d_i^{(c)})_{i \in B_c}, \quad s^{(c)} = (s_i^{(c)})_{i \in B_c}. \tag{2}$$

The reconstruction is therefore subject to three classes of constraints: row sums and column sums derived from balance-sheet totals, and a zero-diagonal constraint reflecting the absence of self-lending.

2.2. Inter-Country Totals

Cross-border aggregates are captured by the $(k + 1) \times (k + 1)$ matrix $\Gamma = (\gamma_{c,d})_{c,d \in C \cup \{k+1\}}$, where $C = \{1, \dots, k\}$; the index $k + 1$ denotes the international rest-of-the-world. Residual RoW entries are computed as

$$\gamma_{c,k+1} = \max(\sum_{d \in C} \gamma_{c,d} - \sum_{d \in C} \gamma_{d,c}, 0), \quad \gamma_{k+1,d} = \max(\sum_{c \in C} \gamma_{c,d} - \sum_{c \in C} \gamma_{d,c}, 0). \tag{3}$$

2.3. Revision of Domestic Totals

For $c \neq d$ the foreign debt allocated to country d by bank $i \in B_c$ is

$$f_i^{(c \rightarrow d)} = \gamma_{cd} \frac{d_i^{(c)}}{\sum_{h \in B_c} d_h^{(c)}}. \tag{4}$$

Netting out foreign exposures yields

$$\tilde{d}_i^{(c)} = d_i^{(c)} - \sum_{d \neq c} f_i^{(c \rightarrow d)}, \tilde{s}_i^{(c)} = s_i^{(c)} - \sum_{d \neq c} f_i^{(d \rightarrow c)}. \tag{5}$$

2.4. Domestic Max-Entropy Reconstruction

Each country c solves

$$\begin{aligned} \min_{L^{(c)}} & \sum_{i \neq j} L_{ij}^{(c)} \log L_{ij}^{(c)} \\ \text{s.t.} & \sum_j L_{ij}^{(c)} = \tilde{d}_i^{(c)}, \sum_i L_{ij}^{(c)} = \tilde{s}_j^{(c)}, L_{ii}^{(c)} = 0. \end{aligned} \tag{6}$$

The numerical solution occupies the country c MaxEntropy block; an extra row/column stores the domestic RoW residual.

2.5. Bilateral Bank-to-Bank Foreign Links

Given countries $c \neq d$, liabilities are distributed proportionally:

$$F_{ij}^{(c,d)} = f_i^{(c \rightarrow d)} \frac{s_j^{(d)}}{\sum_{h \in B_d} s_h^{(d)}}. \tag{7}$$

2.6. Assembly of the Global Exposure Matrix

The resulting matrices define a dual-layer network structure. Each domestic block represents the inferred internal topology of a country’s banking system, while the off-diagonal blocks reflect the distribution of cross-border positions across individual institutions. This structure ensures that domestic and international constraints are jointly satisfied, and that no information is duplicated or omitted. Conceptually, the global matrix can be interpreted as the minimal-information multi-country network consistent with all observable aggregates.

The consolidated matrix is as follows:

$$\mathcal{L} = \begin{bmatrix} L^{(1)} & F^{(1,2)} & \dots & F^{(1,k)} & r^{(1)} & p^{(1)} \\ F^{(2,1)} & L^{(2)} & \dots & F^{(2,k)} & r^{(2)} & p^{(2)} \\ \vdots & \vdots & \ddots & \vdots & \vdots & \vdots \\ F^{(k,1)} & F^{(k,2)} & \dots & L^{(k)} & r^{(k)} & p^{(k)} \\ c^{(1)} & c^{(2)} & \dots & c^{(k)} & 0 & p_{dom \rightarrow int} \\ q^{(1)} & q^{(2)} & \dots & q^{(k)} & q_{int \rightarrow dom} & 0 \end{bmatrix}. \tag{8}$$

Here,

$L^{(c)}$ is the domestic maximum-entropy block for country c ;

$F^{(c,d)}$ ($c \neq d$) contains bilateral liabilities from banks in c to banks in d ;

$r^{(c)}$ (column) and $c^{(c)}$ (row) capture, respectively, debts of country- c banks to the domestic rest-of-the-world (RoW_{dom}) and claims of RoW_{dom} on those banks;

$p^{(c)}$ (column) and $q^{(c)}$ (row) record analogous positions vis-à-vis the international rest-of-the-world (RoW_{int}).

This structure reconciles every row and column total by allocating the unmatched part of each balance sheet either to RoW_{dom} or to RoW_{int} . The two scalar entries, $p_{dom \rightarrow int}$ and $q_{int \rightarrow dom}$, at the intersection of the domestic and international rest-of-the-world tiers serve solely to close any residual imbalance between the two layers. Their exact definitions are:

$$p_{dom \rightarrow int} := \max \left(\sum_{c,i} r_i^{(c)} - \sum_{c,i} c_i^{(c)}, 0 \right)$$

$$q_{int \rightarrow dom} := \max \left(\sum_{c,i} c_i^{(c)} - \sum_{c,i} r_i^{(c)}, 0 \right)$$

In our implementation, both expressions evaluate to zero because each country vector $r^{(c)}$ is constructed by precisely netting foreign exposures out of the original balance-sheet totals, and the international vectors $p^{(c)}$ and $q^{(c)}$ are derived from an already balanced country-to-country matrix. Hence, the domestic and international RoW tiers do not hold claims on each other numerically. The scalars are retained in the analytical form of the block matrix to guarantee consistency under alternative parametrizations—for instance, when inputs are rounded, manually adjusted, or extended so that the domestic RoW can lend abroad. Whenever the balance-sheet closure is perfect, the two corner entries simply take the value 0 and disappear from the numerical matrix without affecting any subsequent simulation.

Unlike existing interbank reconstruction methods that operate either at the domestic level (using maximum-entropy or alternative heuristics) or at the aggregate international level (using country-to-country matrices), the proposed framework integrates these two layers within a single coherent structure. The method preserves the strengths of domestic maximum-entropy reconstruction while incorporating cross-border constraints that domestic models ignore. Conversely, international contagion models based on country aggregates cannot allocate exposures at the bank level. The present framework bridges this gap by producing a multi-country, bank-resolved exposure matrix that cannot be generated by existing approaches.

3. Example of the Model Application

The numerical example illustrates how the reconstruction framework aligns domestic balance-sheet totals with cross-border exposures to obtain an economically coherent multi-country network. Each block of the final matrix carries a specific interpretation: domestic blocks represent inferred internal lending structures consistent with bank size and balance-sheet positions, while off-diagonal blocks capture how each country's external liabilities are allocated across its resident banks. The example therefore demonstrates how cross-border aggregates constrain domestic structures and modify each country's exposure profile.

The accompanying example workbook instantiates the multi-country algorithm for three countries (Belgium, Ireland and Greece) and twenty-eight banks. Each table corresponds directly to one of the analytical objects defined in Sections 2.1–2.6.

We highlight that even if the values are coming from real data,² the purpose of this example is to illustrate the algorithmic steps rather than to perform empirical inference. We highlight that, although the values are drawn from real-world data, the purpose of this example is to illustrate the algorithmic steps of the reconstruction procedure rather than to perform empirical inference. The numerical results are therefore reported to demonstrate the internal accounting consistency of the reconstructed matrix, not to support statistical or policy conclusions.

Tables 1–3 report the observed domestic interbank totals (debts and credits) that serve as initial inputs to the reconstruction and provide the vectors $d^{(c)}$ and $s^{(c)}$ defined in Equation (1).

Table 1. Belgium total exposures.

| | Debts | Credits |
|------------|------------|-----------|
| Belgium 1 | 3,710,000 | 3,874,000 |
| Belgium 2 | 12,852,000 | 2,438,000 |
| Belgium 3 | 307,122 | 144,645 |
| Belgium 4 | 12,403,418 | 3,623,282 |
| Belgium 5 | 4681 | 145,109 |
| Belgium 6 | 288,313 | 776,978 |
| Belgium 7 | 2,788,632 | 430,037 |
| Belgium 8 | 157,381 | 450,175 |
| Belgium 9 | 222 | 17,899 |
| Belgium 10 | 179,634 | 285,719 |
| Belgium 11 | 14,048 | 92,215 |
| Belgium 12 | 0 | 369,832 |
| Belgium 13 | 2657 | 975,578 |
| Belgium 14 | 173,614 | 264,795 |
| Belgium 15 | 451,230 | 99,486 |

Source: Orbis Bank Focus.

Table 2. Greece total exposures.

| | Debts | Credits |
|----------|-----------|-----------|
| Greece 1 | 273,000 | 1,616,000 |
| Greece 2 | 1,560,000 | 2,679,000 |
| Greece 3 | 3,415,000 | 1,311,000 |
| Greece 4 | 101,107 | 77,710 |
| Greece 5 | 0 | 127,650 |
| Greece 6 | 1804 | 7985 |
| Greece 7 | 2043 | 2380 |
| Greece 8 | 3616 | 29,849 |

Source: Orbis Bank Focus.

Table 3. Ireland total exposures.

| | Debts | Credits |
|-----------|------------|-----------|
| Ireland 1 | 14,384,451 | 1,901,050 |
| Ireland 2 | 1,637,000 | 732,000 |
| Ireland 3 | 1,157,000 | 1,115,000 |
| Ireland 4 | 364,231 | 820,574 |
| Ireland 5 | 2,720,869 | 144,087 |

Source: Orbis Bank Focus.

Table 4 represents the $(k + 1) \times (k + 1)$ matrix Γ of Section 2.2. Cell formulas implement the residual rules explained in Section 2.2, ensuring that the external rest-of-the-world row and column balance the observable country aggregates.

Table 4. International exposures.

| | Belgium | Greece | Ireland |
|----------------|---------|--------|-----------|
| Belgium | 0 | 0 | 187,392 |
| Greece | 166,130 | 0 | 1,024,771 |
| Ireland | 382,281 | 0 | 0 |

Source: BIS.

The international exposure components defined in Equation (4) are computed by allocating each country’s aggregate cross-border liabilities across resident banks in proportion to their domestic debt shares. These bank-level foreign components are then netted out from the original balance-sheet positions as described in Equation (5), yielding the revised domestic totals reported in Tables 5–7. These sheets, therefore, allocate international liabilities at the bank level.

Table 5. Belgium revised totals.

| | Debts | Credits |
|------------|------------|-----------|
| Belgium 1 | 3,648,961 | 3,722,114 |
| Belgium 2 | 12,640,552 | 2,342,415 |
| Belgium 3 | 302,069 | 138,974 |
| Belgium 4 | 12,199,351 | 3,481,226 |
| Belgium 5 | 4604 | 139,420 |
| Belgium 6 | 283,570 | 746,515 |
| Belgium 7 | 2,742,752 | 413,177 |
| Belgium 8 | 154,792 | 432,525 |
| Belgium 9 | 218 | 17,197 |
| Belgium 10 | 176,679 | 274,517 |
| Belgium 11 | 13,817 | 88,600 |
| Belgium 12 | 0 | 355,332 |
| Belgium 13 | 2613 | 937,329 |
| Belgium 14 | 170,758 | 254,413 |
| Belgium 15 | 443,806 | 95,586 |

Table 6. Greece revised totals.

| | Debts | Credits |
|----------|-----------|-----------|
| Greece 1 | 212,305 | 1,287,115 |
| Greece 2 | 1,213,173 | 2,133,775 |
| Greece 3 | 2,655,759 | 1,044,188 |
| Greece 4 | 78,628 | 61,895 |
| Greece 5 | 0 | 101,671 |
| Greece 6 | 1403 | 6360 |
| Greece 7 | 1589 | 1896 |
| Greece 8 | 2812 | 23,774 |

Table 7. Ireland revised totals.

| | Debts | Credits |
|-----------|------------|-----------|
| Ireland 1 | 13,523,975 | 1,412,078 |
| Ireland 2 | 1,539,075 | 543,721 |
| Ireland 3 | 1,087,788 | 828,209 |
| Ireland 4 | 342,443 | 609,513 |
| Ireland 5 | 2,558,107 | 107,026 |

Belgium Revised Totals, Greece Revised Totals and Ireland Revised Totals implement Equation (5). Foreign liabilities and claims are netted out to produce the revised domestic vectors $\tilde{d}_i^{(c)}$ and $\tilde{s}_i^{(c)}$, which feed the maximum-entropy optimization.

The revised totals, obtained by subtracting the allocated cross-border components, reflect how foreign positions alter the domestic exposure capacity of each bank and form the row and column constraints for the maximum-entropy reconstruction.

Tables 8–10 contain the numerical solution of the optimization problem (Section 2.4). Rows and columns match the revised totals, and the additional RoW row/column records any domestic residual $r^{(c)}$, $c^{(c)}$.

Table 8. Belgium MaxEntropy.

| | B1 | B2 | B3 | B4 | B5 | B6 | B7 | B8 | B9 | B10 | B11 | B12 | B13 | B14 | B15 | RoW |
|------------|-----------|-----------|-----------|-----------|-----------|-----------|-----------|-----------|-----------|------------|------------|------------|------------|------------|------------|------------|
| B1 | 0 | 421,219 | 15,599 | 635,608 | 15,522 | 83,759 | 49,731 | 48,354 | 1914 | 30,708 | 9867 | 39,556 | 104,353 | 28,454 | 10,770 | 2,153,546 |
| B2 | 1,595,494 | 0 | 53,378 | 2,174,997 | 53,116 | 286,618 | 170,174 | 165,465 | 6551 | 105,079 | 33,763 | 135,358 | 357,087 | 97,368 | 36,855 | 7,369,250 |
| B3 | 34,355 | 31,036 | 0 | 46,833 | 1144 | 6172 | 3664 | 3563 | 141 | 2263 | 727 | 2915 | 7689 | 2097 | 794 | 158,678 |
| B4 | 1,634,678 | 1,476,773 | 54,689 | 0 | 54,421 | 293,657 | 174,353 | 169,528 | 6712 | 107,660 | 34,592 | 138,682 | 365,856 | 99,759 | 37,761 | 7,550,230 |
| B5 | 524 | 473 | 18 | 714 | 0 | 94 | 56 | 54 | 2 | 34 | 11 | 44 | 117 | 32 | 12 | 2418 |
| B6 | 32,796 | 29,628 | 1097 | 44,708 | 1092 | 0 | 3498 | 3401 | 135 | 2160 | 694 | 2782 | 7340 | 2001 | 758 | 151,479 |
| B7 | 314,557 | 284,172 | 10,524 | 428,808 | 10,472 | 56,508 | 0 | 32,622 | 1292 | 20,717 | 6657 | 26,686 | 70,401 | 19,196 | 7266 | 1,452,874 |
| B8 | 17,747 | 16,032 | 594 | 24,192 | 591 | 3188 | 1893 | 0 | 73 | 1169 | 376 | 1506 | 3972 | 1083 | 410 | 81,968 |
| B9 | 25 | 22 | 1 | 34 | 1 | 4 | 3 | 3 | 0 | 2 | 1 | 2 | 6 | 2 | 1 | 114 |
| B10 | 20,168 | 18,220 | 675 | 27,494 | 671 | 3623 | 2151 | 2092 | 83 | 0 | 427 | 1711 | 4514 | 1231 | 466 | 93,153 |
| B11 | 1569 | 1418 | 52 | 2139 | 52 | 282 | 167 | 163 | 6 | 103 | 0 | 133 | 351 | 96 | 36 | 7248 |
| B12 | 0 | 0 | 0 | 0 | 0 | 0 | 0 | 0 | 0 | 0 | 0 | 0 | 0 | 0 | 0 | 0 |
| B13 | 304 | 274 | 10 | 414 | 10 | 55 | 32 | 32 | 1 | 20 | 6 | 26 | 0 | 19 | 7 | 1403 |
| B14 | 19,482 | 17,600 | 652 | 26,558 | 649 | 3500 | 2078 | 2020 | 80 | 1283 | 412 | 1653 | 4360 | 0 | 450 | 89,982 |
| B15 | 50,416 | 45,546 | 1687 | 68,727 | 1678 | 9057 | 5377 | 5228 | 207 | 3320 | 1067 | 4277 | 11,283 | 3077 | 0 | 232,859 |
| RoW | 0 | 0 | 0 | 0 | 0 | 0 | 0 | 0 | 0 | 0 | 0 | 0 | 0 | 0 | 0 | 0 |

Table 9. Greece MaxEntropy.

| | G 1 | G 2 | G 3 | G 4 | G 5 | G 6 | G 7 | G 8 | RoW |
|------------|------------|------------|------------|------------|------------|------------|------------|------------|------------|
| G 1 | 0 | 113,329 | 91,706 | 2319 | 3766 | 236 | 70 | 881 | 0 |
| G 2 | 404,493 | 0 | 749,272 | 18,943 | 30,768 | 1925 | 574 | 7197 | 0 |
| G 3 | 772,919 | 1,769,322 | 0 | 36,198 | 58,793 | 3678 | 1096 | 13,753 | 0 |
| G 4 | 15,001 | 34,339 | 27,787 | 0 | 1141 | 71 | 21 | 267 | 0 |
| G 5 | 0 | 0 | 0 | 0 | 0 | 0 | 0 | 0 | 0 |
| G 6 | 266 | 608 | 492 | 12 | 20 | 0 | 0 | 5 | 0 |
| G 7 | 301 | 688 | 557 | 14 | 23 | 1 | 0 | 5 | 0 |
| G 8 | 534 | 1221 | 988 | 25 | 41 | 3 | 1 | 0 | 0 |
| RoW | 93,602 | 214,268 | 173,386 | 4384 | 7120 | 445 | 133 | 1666 | 0 |

Table 10. Ireland MaxEntropy.

| | I 1 | I 2 | I 3 | I 4 | I 5 | RoW |
|------------|------------|------------|------------|------------|------------|------------|
| I 1 | 0 | 444,047 | 662,927 | 471,613 | 91,519 | 11,853,869 |
| I 2 | 395,761 | 0 | 57,946 | 41,224 | 8000 | 1,036,144 |
| I 3 | 283,237 | 27,778 | 0 | 29,503 | 5725 | 741,545 |
| I 4 | 88,195 | 8650 | 12,913 | 0 | 1783 | 230,903 |
| I 5 | 644,886 | 63,247 | 94,423 | 67,173 | 0 | 1,688,379 |
| RoW | 0 | 0 | 0 | 0 | 0 | 0 |

The domestic maximum-entropy blocks reflect the least-biased internal distribution of exposures consistent with the revised totals. This generates diversified domestic linkages, illustrating how the country’s internal interbank network adjusts once cross-border constraints are imposed.

Table 11 assembles all blocks according to the structure shown in Equation (8). It therefore reconciles domestic and cross-border components into a coherent multi-country network consistent with all observable aggregates.

Table 11. Final matrix.

| | B1 | B2 | B3 | B4 | B5 | B6 | B7 | B8 | B9 | B10 | B11 | B12 | B13 | B14 | B15 |
|------------|------------|------------|------------|------------|------------|------------|------------|------------|------------|------------|------------|------------|------------|------------|------------|
| B1 | 0 | 421,219 | 15,599 | 635,608 | 15,522 | 83,759 | 49,731 | 48,354 | 1914 | 30,708 | 9867 | 39,556 | 104,353 | 28,454 | 10,770 |
| B2 | 1,595,494 | 0 | 53,378 | 2,174,997 | 53,116 | 286,618 | 170,174 | 165,465 | 6551 | 105,079 | 33,763 | 135,358 | 357,087 | 97,368 | 36,855 |
| B3 | 34,355 | 31,036 | 0 | 46,833 | 1144 | 6172 | 3664 | 3563 | 141 | 2263 | 727 | 2915 | 7689 | 2097 | 794 |
| B4 | 1,634,678 | 1,476,773 | 54,689 | 0 | 54,421 | 293,657 | 174,353 | 169,528 | 6712 | 107,660 | 34,592 | 138,682 | 365,856 | 99,759 | 37,761 |
| B5 | 524 | 473 | 18 | 714 | 0 | 94 | 56 | 54 | 2 | 34 | 11 | 44 | 117 | 32 | 12 |
| B6 | 32,796 | 29,628 | 1097 | 44,708 | 1092 | 0 | 3498 | 3401 | 135 | 2160 | 694 | 2782 | 7340 | 2001 | 758 |
| B7 | 314,557 | 284,172 | 10,524 | 428,808 | 10,472 | 56,508 | 0 | 32,622 | 1292 | 20,717 | 6657 | 26,686 | 70,401 | 19,196 | 7266 |
| B8 | 17,747 | 16,032 | 594 | 24,192 | 591 | 3188 | 1893 | 0 | 73 | 1169 | 376 | 1506 | 3972 | 1083 | 410 |
| B9 | 25 | 22 | 1 | 34 | 1 | 4 | 3 | 3 | 0 | 2 | 1 | 2 | 6 | 2 | 1 |
| B10 | 20,168 | 18,220 | 675 | 27,494 | 671 | 3623 | 2151 | 2092 | 83 | 0 | 427 | 1711 | 4514 | 1231 | 466 |
| B11 | 1569 | 1418 | 52 | 2139 | 52 | 282 | 167 | 163 | 6 | 103 | 0 | 133 | 351 | 96 | 36 |
| B12 | 0 | 0 | 0 | 0 | 0 | 0 | 0 | 0 | 0 | 0 | 0 | 0 | 0 | 0 | 0 |
| B13 | 304 | 274 | 10 | 414 | 10 | 55 | 32 | 32 | 1 | 20 | 6 | 26 | 0 | 19 | 7 |
| B14 | 19,482 | 17,600 | 652 | 26,558 | 649 | 3500 | 2078 | 2020 | 80 | 1283 | 412 | 1653 | 4360 | 0 | 450 |
| B15 | 50,416 | 45,546 | 1687 | 68,727 | 1678 | 9057 | 5377 | 5228 | 207 | 3320 | 1067 | 4277 | 11,283 | 3077 | 0 |
| G 1 | 2345 | 1476 | 88 | 2193 | 88 | 470 | 260 | 272 | 11 | 173 | 56 | 224 | 591 | 160 | 60 |
| G 2 | 13,400 | 8433 | 500 | 12,533 | 502 | 2687 | 1487 | 1557 | 62 | 988 | 319 | 1279 | 3374 | 916 | 344 |
| G 3 | 29,333 | 18,460 | 1095 | 27,435 | 1099 | 5883 | 3256 | 3409 | 136 | 2163 | 698 | 2800 | 7387 | 2005 | 753 |
| G 4 | 868 | 547 | 32 | 812 | 33 | 174 | 96 | 101 | 4 | 64 | 21 | 83 | 219 | 59 | 22 |
| G 5 | 0 | 0 | 0 | 0 | 0 | 0 | 0 | 0 | 0 | 0 | 0 | 0 | 0 | 0 | 0 |
| G 6 | 15 | 10 | 1 | 14 | 1 | 3 | 2 | 2 | 0 | 1 | 0 | 1 | 4 | 1 | 0 |
| G 7 | 18 | 11 | 1 | 16 | 1 | 4 | 2 | 2 | 0 | 1 | 0 | 2 | 4 | 1 | 0 |
| G 8 | 31 | 20 | 1 | 29 | 1 | 6 | 3 | 4 | 0 | 2 | 1 | 3 | 8 | 2 | 1 |
| I 1 | 75,157 | 47,298 | 2806 | 70,293 | 2815 | 15,074 | 8343 | 8734 | 347 | 5543 | 1789 | 7175 | 18,927 | 5137 | 1930 |
| I 2 | 8553 | 5383 | 319 | 8000 | 320 | 1715 | 949 | 994 | 40 | 631 | 204 | 817 | 2154 | 585 | 220 |
| I 3 | 6045 | 3804 | 226 | 5654 | 226 | 1212 | 671 | 702 | 28 | 446 | 144 | 577 | 1522 | 413 | 155 |
| I 4 | 1903 | 1198 | 71 | 1780 | 71 | 382 | 211 | 221 | 9 | 140 | 45 | 182 | 479 | 130 | 49 |
| I 5 | 14,216 | 8947 | 531 | 13,296 | 533 | 2851 | 1578 | 1652 | 66 | 1048 | 338 | 1357 | 3580 | 972 | 365 |
| R d | 0 | 0 | 0 | 0 | 0 | 0 | 0 | 0 | 0 | 0 | 0 | 0 | 0 | 0 | 0 |
| R i | 0 | 0 | 0 | 0 | 0 | 0 | 0 | 0 | 0 | 0 | 0 | 0 | 0 | 0 | 0 |
| | G 1 | G 2 | G 3 | G 4 | G 5 | G 6 | G 7 | G 8 | I 1 | I 2 | I 3 | I 4 | I 5 | R d | R i |
| B1 | 0 | 0 | 0 | 0 | 0 | 0 | 0 | 0 | 8413 | 3240 | 4935 | 3632 | 638 | 2,153,546 | 40,182 |
| B2 | 0 | 0 | 0 | 0 | 0 | 0 | 0 | 0 | 29,145 | 11,222 | 17,094 | 12,580 | 2209 | 7,369,250 | 139,196 |
| B3 | 0 | 0 | 0 | 0 | 0 | 0 | 0 | 0 | 696 | 268 | 409 | 301 | 53 | 158,678 | 3326 |
| B4 | 0 | 0 | 0 | 0 | 0 | 0 | 0 | 0 | 28,128 | 10,831 | 16,498 | 12,141 | 2132 | 7,550,230 | 134,338 |
| B5 | 0 | 0 | 0 | 0 | 0 | 0 | 0 | 0 | 11 | 4 | 6 | 5 | 1 | 2418 | 51 |
| B6 | 0 | 0 | 0 | 0 | 0 | 0 | 0 | 0 | 654 | 252 | 383 | 282 | 50 | 151,479 | 3123 |

Table 11. *Cont.*

| | G 1 | G 2 | G 3 | G 4 | G 5 | G 6 | G 7 | G 8 | I 1 | I 2 | I 3 | I 4 | I 5 | R d | R i | |
|------------|------------|------------|------------|------------|------------|------------|------------|------------|------------|------------|------------|------------|------------|------------|------------|--------|
| B7 | 0 | 0 | 0 | 0 | 0 | 0 | 0 | 0 | 0 | 6324 | 2435 | 3709 | 2730 | 479 | 1,452,874 | 30,203 |
| B8 | 0 | 0 | 0 | 0 | 0 | 0 | 0 | 0 | 0 | 357 | 137 | 209 | 154 | 27 | 81,968 | 1705 |
| B9 | 0 | 0 | 0 | 0 | 0 | 0 | 0 | 0 | 0 | 1 | 0 | 0 | 0 | 0 | 114 | 2 |
| B10 | 0 | 0 | 0 | 0 | 0 | 0 | 0 | 0 | 0 | 407 | 157 | 239 | 176 | 31 | 93,153 | 1946 |
| B11 | 0 | 0 | 0 | 0 | 0 | 0 | 0 | 0 | 0 | 32 | 12 | 19 | 14 | 2 | 7248 | 152 |
| B12 | 0 | 0 | 0 | 0 | 0 | 0 | 0 | 0 | 0 | 0 | 0 | 0 | 0 | 0 | 0 | 0 |
| B13 | 0 | 0 | 0 | 0 | 0 | 0 | 0 | 0 | 0 | 6 | 2 | 4 | 3 | 0 | 1403 | 29 |
| B14 | 0 | 0 | 0 | 0 | 0 | 0 | 0 | 0 | 0 | 394 | 152 | 231 | 170 | 30 | 89,982 | 1880 |
| B15 | 0 | 0 | 0 | 0 | 0 | 0 | 0 | 0 | 0 | 1023 | 394 | 600 | 442 | 78 | 232,859 | 4887 |
| G 1 | 0 | 113,329 | 91,706 | 2319 | 3766 | 236 | 70 | 881 | 21,068 | 8112 | 12,357 | 9094 | 1597 | 0 | 0 | 0 |
| G 2 | 404,493 | 0 | 749,272 | 18,943 | 30,768 | 1925 | 574 | 7197 | 120,389 | 46,356 | 70,610 | 51,965 | 9125 | 0 | 0 | 0 |
| G 3 | 772,919 | 1,769,322 | 0 | 36,198 | 58,793 | 3678 | 1096 | 13,753 | 263,544 | 101,478 | 154,573 | 113,757 | 19,975 | 0 | 0 | 0 |
| G 4 | 15,001 | 34,339 | 27,787 | 0 | 1141 | 71 | 21 | 267 | 7803 | 3004 | 4576 | 3368 | 591 | 0 | 0 | 0 |
| G 5 | 0 | 0 | 0 | 0 | 0 | 0 | 0 | 0 | 0 | 0 | 0 | 0 | 0 | 0 | 0 | 0 |
| G 6 | 266 | 608 | 492 | 12 | 20 | 0 | 0 | 5 | 139 | 54 | 82 | 60 | 11 | 0 | 0 | 0 |
| G 7 | 301 | 688 | 557 | 14 | 23 | 1 | 0 | 5 | 158 | 61 | 92 | 68 | 12 | 0 | 0 | 0 |
| G 8 | 534 | 1221 | 988 | 25 | 41 | 3 | 1 | 0 | 279 | 107 | 164 | 120 | 21 | 0 | 0 | 0 |
| I 1 | 0 | 0 | 0 | 0 | 0 | 0 | 0 | 0 | 0 | 444,047 | 662,927 | 471,613 | 91,519 | 11,853,869 | 589,107 | 0 |
| I 2 | 0 | 0 | 0 | 0 | 0 | 0 | 0 | 0 | 395,761 | 0 | 57,946 | 41,224 | 8000 | 1,036,144 | 67,042 | 0 |
| I 3 | 0 | 0 | 0 | 0 | 0 | 0 | 0 | 0 | 283,237 | 27,778 | 0 | 29,503 | 5725 | 741,545 | 47,384 | 0 |
| I 4 | 0 | 0 | 0 | 0 | 0 | 0 | 0 | 0 | 88,195 | 8650 | 12,913 | 0 | 1783 | 230,903 | 14,917 | 0 |
| I 5 | 0 | 0 | 0 | 0 | 0 | 0 | 0 | 0 | 644,886 | 63,247 | 94,423 | 67,173 | 0 | 1,688,379 | 111,432 | 0 |
| R d | 93,602 | 214,268 | 173,386 | 4384 | 7120 | 445 | 133 | 1666 | 0 | 0 | 0 | 0 | 0 | 0 | 0 | 0 |
| R i | 328,885 | 545,225 | 266,812 | 15,815 | 25,979 | 1625 | 484 | 6075 | 0 | 0 | 0 | 0 | 0 | 0 | 0 | 0 |

Off-diagonal blocks import the bilateral foreign liabilities $F^{(c,d)}$ derived in Section 2.6, diagonal blocks import the domestic matrices $L^{(c)}$, and the two RoW tiers occupy the last two indices. As the calibration is internally balanced, the corner scalars $p_{\text{dom} \rightarrow \text{int}}$ and $q_{\text{int} \rightarrow \text{dom}}$ defined after Equation (8) evaluate to zero, leaving those cells empty.

The final matrix shows how the multi-country network emerges as a coherent aggregation of domestic and cross-border structures: off-diagonal blocks quantify bilateral interconnectedness between countries, while the RoW layers capture residual exposures to non-modelled counterparts. The resulting topology can support contagion simulations by indicating which countries and institutions are most exposed to foreign shocks.

Such a matrix can serve as an input for a variety of contagion and stress-testing models, enabling analyses of how domestic fragilities propagate internationally and how cross-border liabilities shape systemic risk contributions. By linking bank-level balance-sheet positions with country-level aggregates, the framework supports more realistic multi-country contagion assessments.

Taken together, these tables provide a complete, numerically consistent instantiation of the analytical framework: every worksheet maps to a specific equation, and the flow of references mirrors the logical progression of the algorithm from raw inputs to the consolidated inter-bank liability matrix \mathcal{L} .

Overall, the example highlights how cross-border aggregates reshape the domestic exposure landscape and determine the distribution of foreign claims among resident institutions. The reconstructed network therefore provides insight into which banks act as principal channels of international transmission, how domestic diversification interacts with foreign exposures, and how multi-country contagion mechanisms may arise. Although the example is synthetic, the structure it produces mirrors the economic logic of globally connected banking systems.

To test the actual effects on contagion estimates, we performed a simulation exercise based on the SYMBOL model, firstly developed by De Lisa et al. (2011), then adopted by the European Commission as a standard tool for shaping and backtesting the European banking regulation (see European Commission, 2011a, 2011b, 2016; Benczur et al., 2017).

To disentangle the idiosyncratic and contagion risk contributions of each bank, we performed the simulation both with and without allowing contagion effects. We then considered the net contagion effects obtained as the difference among total (with contagion) risk contributions and no contagion risk contributions.

The “with contagion” estimates were performed in two different configurations of the international interbank matrices: the first was obtained with maximum entropy, as if all banks were part of a single country (as in Benczur et al., 2017), and the second was obtained by the method described above, which considers the BIS data on international exposures.

The results reported in Table 12 show that contagion effects are very different in the two estimates. Some examples include Belgium bank 4, whose net contagion contribution increases from 27.32 to 95.99, and Ireland bank 2, whose net contagion contribution decreases from 22.23 to 3.22.

These differences highlight how incorporating cross-border information at the bank level can materially alter estimated contagion contributions, even when the underlying balance-sheet data are unchanged. The purpose of this comparison is methodological validation rather than regulatory calibration or policy inference.

Table 12. Risk contributions by bank.

| | No Interbank Contagion | Total Contributions with Contagion | | Net Contagion Contributions | |
|------------|------------------------|------------------------------------|---------|-----------------------------|--------|
| | | Max Entropy | BIS | Max Entropy | BIS |
| Belgium 1 | 4679.76 | 4686.96 | 4707.27 | 7.20 | 27.51 |
| Belgium 2 | 2999.56 | 3020.53 | 3053.17 | 20.97 | 53.62 |
| Belgium 3 | 2258.42 | 2259.00 | 2259.14 | 0.58 | 0.72 |
| Belgium 4 | 1719.05 | 1746.37 | 1815.04 | 27.32 | 95.99 |
| Belgium 5 | 90.99 | 90.99 | 90.99 | 0.00 | 0.00 |
| Belgium 6 | 45.91 | 45.91 | 45.91 | 0.00 | 0.00 |
| Belgium 8 | 1302.75 | 1347.60 | 1440.65 | 44.85 | 137.90 |
| Belgium 9 | 6.15 | 6.16 | 6.16 | 0.00 | 0.01 |
| Belgium 10 | 12.28 | 12.28 | 12.28 | 0.00 | 0.00 |
| Belgium 11 | 19.94 | 20.03 | 20.09 | 0.10 | 0.16 |
| Belgium 12 | 7.02 | 7.03 | 7.04 | 0.01 | 0.01 |
| Belgium 13 | 68.20 | 68.20 | 68.20 | 0.00 | 0.00 |
| Belgium 14 | 0.23 | 0.23 | 0.23 | 0.00 | 0.00 |
| Belgium 15 | 0.20 | 0.21 | 0.21 | 0.01 | 0.01 |
| Greece 1 | 23.15 | 25.52 | 31.36 | 2.36 | 8.21 |
| Greece 2 | 791.72 | 792.13 | 793.11 | 0.41 | 1.39 |
| Greece 3 | 448.56 | 449.84 | 455.57 | 1.28 | 7.01 |
| Greece 4 | 1456.39 | 1462.99 | 1472.75 | 6.60 | 16.37 |
| Greece 5 | 397.23 | 397.78 | 398.32 | 0.56 | 1.10 |
| Greece 6 | 1.22 | 1.22 | 1.22 | 0.00 | 0.00 |
| Greece 7 | 34.34 | 34.35 | 34.35 | 0.01 | 0.01 |
| Greece 8 | 9.77 | 9.77 | 9.77 | 0.00 | 0.01 |
| Ireland 1 | 1.21 | 1.21 | 1.21 | 0.00 | 0.00 |
| Ireland 2 | 1353.00 | 1375.22 | 1356.22 | 22.23 | 3.22 |
| Ireland 3 | 564.34 | 565.24 | 565.57 | 0.90 | 1.22 |
| Ireland 4 | 1411.60 | 1412.47 | 1412.08 | 0.86 | 0.48 |
| Ireland 5 | 86.55 | 86.74 | 86.68 | 0.19 | 0.13 |

4. Conclusions

In this paper we developed an algorithm that integrates total interbank credits and debts from financial statements with international country-to-country exposures, producing a consistent multi-country interbank matrix suitable for contagion analysis.

The step-by-step presentation adopted in the example is intentional, allowing readers to trace the construction of the multi-country matrix and understand how each component contributes to the final network.

The illustrative example shows that the framework produces a globally consistent exposure matrix in which domestic and cross-border constraints are jointly satisfied, demonstrating that the approach operationally integrates multi-country information into a coherent network structure. The approach, however, inherits the limitations of maximum-entropy reconstructions and relies on the availability of aggregate cross-border exposures.

This integration, based on a dual-layer interbank network, overcomes previous models' country-segmentation assumption while embedding global financial interconnectedness, and provides a tool for more accurate assessment of financial contagion risks and systemic risk levels.

It does so by linking each country's domestic maximum-entropy block to the cross-border exposure constraints imposed by other countries, ensuring that domestic matrices are not reconstructed in isolation but jointly determined within a global network. In previous models, domestic exposure matrices were estimated independently for each country, ignoring how cross-border liabilities affect the feasible set of domestic exposures.

Our framework explicitly embeds these international constraints, ensuring that the row and column totals of each country are consistent with cross-country flows.

The present contribution establishes the methodological basis for integrating domestic and cross-country structures in systemic-risk analysis, by improving the internal coherence of multi-country exposure estimates and providing a consistent input for contagion simulations and systemic risk analysis.

Author Contributions: All authors have equally contributed to this work. All authors have read and agreed to the published version of the manuscript.

Funding: This study received funding from the European Union-Next-GenerationEU-National Recovery and Resilience Plan (NRRP)–MISSION 4 COMPONENT 2, INVESTMENT N. 1.1, CALL PRIN 2022 PNRR D.D. 1409 14-09-2022–Incorporating climate-related risks into financial stability assessments: where are we now and how can we move forward? CUP N. P2022WM82K.

Institutional Review Board Statement: Not applicable.

Informed Consent Statement: Not applicable.

Data Availability Statement: The input data used for this exercise are not available as coming from Orbis Bank Focus.

Conflicts of Interest: The authors declare no conflicts of interest.

Notes

- ¹ Other approaches have developed qualified estimations of bank default risks, mainly based on linear regressions (starting from Altman, 1968), or on discriminant models (e.g., Gaul & Jones, 2021), but these approaches are neither intended nor able to estimate contagion risks, and thus are not considered in this paper.
- ² Data coming from Orbis Bank Focus for 2024.

References

- Acemoglu, D., Ozdaglar, A., & Tahbaz-Salehi, A. (2015). Systemic risk and stability in financial networks. *American Economic Review*, 105, 564–608. [CrossRef]
- Acharya, V. V., & Yorulmazer, T. (2010). Information contagion and bank herding. *Journal of Money, Credit and Banking*, 40(1), 215–231. [CrossRef]
- Adrian, T., & Brunnermeier, M. K. (2016). CoVaR. *The American Economic Review*, 106(7), 1705. [CrossRef]
- Aldasoro, I., Gatti, D. D., & Faia, E. (2015). *Bank networks: Contagion, systemic risk and prudential policy* (CESifo Working Paper Series NO. 5182). Available online: https://www.ifo.de/DocDL/cesifo1_wp5182.pdf (accessed on 28 January 2026).
- Allen, F., & Gale, D. (2000). Financial contagion. *Journal of Political Economy*, 108, 1–33. [CrossRef]
- Altman, E. I. (1968). Financial ratios, discriminant analysis and the prediction of corporate bankruptcy. *The Journal of Finance*, 23, 589–609. [CrossRef]
- Battiston, S., Puliga, M., Kaushik, R., Tasca, P., & Caldarelli, G. (2012). DebtRank: Too central to fail? Financial networks, the FED and systemic risk. *Scientific Reports*, 2(1), 541. [CrossRef]
- Benczur, P., Cannas, G., Cariboni, J., Di Girolamo, F., Maccaferri, S., & Petracco Giudici, M. (2017). Evaluating the effectiveness of the new EU bank regulatory framework: A farewell to bail-out? *Journal of Financial Stability*, 33(12), 207223. [CrossRef]
- Benoit, S., Colliard, J. E., & Hurlin, C. (2017). Where the risks lie: A survey on systemic risk. *Review of Finance*, 1, 109–152. [CrossRef]
- Blien, U., & Graef, F. (1997). Entropy optimization methods for the estimation of tables. In I. Balderjahn, R. Mathar, & M. Schader (Eds.), *Classification, data analysis, and data highways* (pp. 3–15). Springer.
- Bostanci, G., & Yilmaz, K. (2020). How connected is the global sovereign credit risk network? *Journal of Banking and Finance*, 113, 105761. [CrossRef]
- Brownlees, C., & Engle, R. F. (2017). SRISK: A conditional capital shortfall measure of systemic risk. *The Review of Financial Studies*, 30, 48–79. [CrossRef]
- Brunnermeier, M., Gorton, G., & Krishnamurthy, A. (2009). *Liquidity mismatch measurement, risk topography: Systemic risk and macro modeling*. University of Chicago Press.
- Brusco, S., & Castiglionesi, F. (2007). Liquidity coinsurance, moral hazard and financial contagion. *Journal of Finance*, 62, 2275–2302. [CrossRef]

- Cifuentes, R., Ferrucci, G., & Shin, H. S. (2005). Liquidity risk and contagion. *Journal of the European Economic Association*, 3(2–3), 556–566. [\[CrossRef\]](#)
- Davidović, S., Kothiyal, A., Galešić, M., Katsikopoulos, K., & Arinaminpathy, N. (2019). Liquidity hoarding in financial networks: The role of structure uncertainty. *Complexity*, 2019, 8436505. [\[CrossRef\]](#)
- Davydov, D., Vahamaa, S., & Yasar, S. (2021). Banking liquidity creation and systemic risk. *Journal of Banking & Finance*, 123, 106031. [\[CrossRef\]](#)
- De Lisa, R., Zedda, S., Vallascas, F., Campolongo, F., & Marchesi, M. (2011). Modelling deposit insurance schemes' losses in a Basel 2 framework. *Journal of Financial Services Research*, 40(3), 123–141. [\[CrossRef\]](#)
- Elliott, M., Golub, B., & Jackson, M. O. (2014). Financial network and contagion. *American Economic Review*, 104, 3115–3153. [\[CrossRef\]](#)
- European Commission. (2011a). Directorate general for economic and financial affairs, Public finances in EMU 2011. *European Economy*, 3, 2011.
- European Commission. (2011b). *Directorate-general for internal market and services: Commission staff working document—Impact assessment accompanying the proposal for a directive of the European parliament and of the council establishing a framework for the recovery and resolution* (SWD(2012) 166 Final). European Commission.
- European Commission. (2016). Directorate-general for financial stability, financial services and capital markets union. In *Effects analysis on the European deposit insurance scheme (EDIS)*. European Commission.
- Freixas, X., Parigi, B., & Rochet, J. C. (2000). Systemic risk, interbank relations and liquidity provision by the central bank. *Journal of Money, Credit and Banking*, 32, 611–638. [\[CrossRef\]](#)
- Gaul, L., & Jones, J. (2021). *CAMELS ratings and their information content*. The Office of the Comptroller of the Currency.
- Glasserman, P. H., & Young, P. (2015). How likely is contagion in financial networks? *Journal of Banking and Finance*, 50(7), 383–399. [\[CrossRef\]](#)
- Hasman, A., & Samartin, M. (2008). Information acquisition and financial contagion. *Journal of Banking & Finance*, 32, 2136–2147. [\[CrossRef\]](#)
- Holopainen, M., & Sarlin, P. (2017). Toward robust early-warning models: A horse race, ensembles and model uncertainty. *Quantitative Finance*, 17, 1933–1963. [\[CrossRef\]](#)
- Huang, X., Zhou, H., & Zhu, H. (2009). A framework for assessing the systemic risk of major financial institutions. *Journal of Banking & Finance*, 33(11), 2036–2049. [\[CrossRef\]](#)
- Karimalis, E. N., & Nomikos, N. K. (2018). Measuring systemic risk in the European banking sector: A copula CoVaR approach. *European Journal of Finance*, 24(2), 944–975. [\[CrossRef\]](#)
- Ladley, D. (2011). Contagion and risk-sharing on the inter-bank market. In *Discussion papers in economics 11/10*. Department of Economics, University of Leicester.
- Levy-Carciente, S., Kenett, D. Y., Avakian, A., Stanley, H. E., & Havlin, S. (2015). Dynamical macroprudential stress testing using network theory. *Journal of Banking & Finance*, 59(1), 164–181. [\[CrossRef\]](#)
- Mistrulli, P. E. (2010). Assessing financial contagion in the interbank market: Maximum entropy versus observed interbank lending patterns. *Journal of Banking & Finance*, 25, 1114–1127.
- Upper, C. (2011). Simulation methods to assess the danger of contagion in interbank markets. *Journal of Financial Stability*, 7, 111–125. [\[CrossRef\]](#)
- Upper, C., & Worms, A. (2004). Estimating bilateral exposures in the German interbank market: Is there a danger of contagion? *European Economic Review*, 48(4), 827–849. [\[CrossRef\]](#)
- Zedda, S., & Cannas, G. (2020). Assessing banks' systemic risk contribution and contagion determinants through the leave-one-out approach. *Journal of Banking and Finance*, 112, 105160. [\[CrossRef\]](#)
- Zedda, S., Cannas, G., & Galliani, C. (2014). The determinants of interbank contagion: Do patterns matter? In *Mathematical and statistical methods for actuarial sciences and finance—MAF 2012*. Springer.
- Zedda, S., & Sbaraglia, S. (2020). Which interbank net is the safest? *Risk Management*, 22, 65–82. [\[CrossRef\]](#)
- Zedda, S., & Spinace-Casale, A. (2021). Modeling and simulating cross country banking contagion risks. *Journal of Risk and Financial Management*, 14(8), 351. [\[CrossRef\]](#)
- Zhang, X., Wei, C., & Zedda, S. (2020). Analysis of China commercial banks' systemic risk sustainability through the leave-one-out approach. *Sustainability*, 12, 203. [\[CrossRef\]](#)

Disclaimer/Publisher's Note: The statements, opinions and data contained in all publications are solely those of the individual author(s) and contributor(s) and not of MDPI and/or the editor(s). MDPI and/or the editor(s) disclaim responsibility for any injury to people or property resulting from any ideas, methods, instructions or products referred to in the content.